AIP | The Journal of Chemical Physics

The Detection of Atoms and Free Radicals in Flames by Mass Spectrometric Techniques

S. N. Foner and R. L. Hudson

Citation: The Journal of Chemical Physics **21**, 1374 (1953); doi: 10.1063/1.1699226
View online: http://dx.doi.org/10.1063/1.1699226
View Table of Contents: http://scitation.aip.org/content/aip/journal/jcp/21/8?ver=pdfcov
Published by the AIP Publishing

THE JOURNAL OF CHEMICAL PHYSICS VOLUME 21, NUMBER 8 AUGUST, 1953

The Detection of Atoms and Free Radicals in Flames by Mass Spectrometric Techniques*

S. N. FONER AND R. L. HUDSON
Applied Physics Laboratory, The Johns Hopkins University, Silver Spring, Maryland

(Received Februrary 13, 1953)

A mass spectrometric method employing a molecular beam gas sampling system has been developed for the detection of atoms and radicals in chemical reactions. Background signals have been virtually eliminated by mechanically modulating the molecular beam and applying phase detection to the ion signal. The application of the method is illustrated by examples of low-pressure flames. In the hydrogen-oxygen flame H, O, and OH have been positively identified. The mass spectrum of a simple hydrocarbon flame, such as the methane-oxygen flame, is complicated by the presence of a large number of stable components generated in the flame. In the methane-oxygen flame the stable intermediates include C_2H_2, CO, CH_2O or C_2H_6, CH_4O, and C_4H_2. The methyl radical has been clearly identified in the methane-oxygen flame. A search for the HO_2 radical in the hydrogen-oxygen flame was made without obtaining positive results. The HO_2 detection problem is discussed in detail.

I. INTRODUCTION

ALTHOUGH there is little doubt that most chemical reactions proceed as chain processes involving atoms and free radicals as intermediates, the specific elementary reactions which take place have been unambiguously established in only a few cases. In the case of combustion reactions the experimental evidence for the existence of atoms and radicals has been fragmentary. Optical spectroscopy of flames has been applied with success to atoms and a number of diatomic radicals such as OH, CH, C_2, and NH. The spectroscopic situation in regard to polyatomic radicals is not very satisfactory because of serious identification difficulties.[1] The spectroscopic method does, however, supply data, unattainable by any other method, on the excited states of the components which it is able to identify.

The difficulties encountered by spectroscopic methods both in detecting radicals and in deriving concentrations from the observed spectral intensities has led to the exploration of other experimental techniques. These include (1) Paneth mirror method, (2) molecular beam methods, (3) mass spectrometry, and (4) microwave spectroscopy.

Of all the methods that have been proposed for studying reaction intermediates, the mass spectrometric method because of inherently high sensitivity, analytical response to all components, and capability of supplying quantitive determinations, appears to offer the greatest promise. The capabilities of the mass spectrometer were explored by Eltenton[2] in studies of the reaction intermediates in the thermal decomposition of some lower hydrocarbons and in low-pressure flames. A number of short-lived intermediates in flames were successfully detected in the pioneering experiments of Eltenton. However, certain expected radicals, such as OH, whose presence is substantiated by prolific spectroscopic data, were not found.

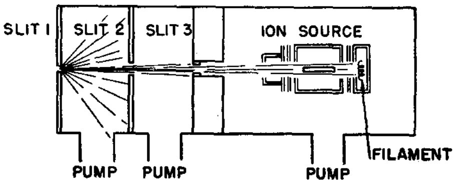

FIG. 1. Schematic diagram of the molecular beam gas sampling system.

II. PRINCIPLE OF THE METHOD

The high reactivity of intermediates occurring in flames places special requirements on the mass spectrometer gas sampling system: (1) the gas sample must be removed from the reaction zone as rapidly as possible; (2) collisions of the gas molecules with the walls of the instrument must be avoided. A hybrid molecular beam type gas sampling system was designed for this purpose and is shown schematically in Fig. 1. Gases from the reaction zone, to the left of Slit 1, stream through the first orifice as a sonic jet, at the usual reaction vessel pressures, with the flow rapidly changing in character from viscous to molecular as the pressure drops. The second slit selects the central portion of the gas stream emerging from the first orifice thereby selecting a sample of gas molecules which had the least likelihood of colliding with the walls of the inlet orifice. Slit 3 by providing additional collimation of the molecular beam is effective in preventing scattered gas molecules in the first gap from entering the ionization chamber of the mass spectrometer. Diffusion pumps evacuate the three sections of the apparatus. The electron beam in the ion source is made coaxial with the molecular beam to increase the probability of ionizing the incoming gas molecules. In certain respects the sampling system resembles the molecular beam system used by Fraser and Jewitt[3] in studying the ionization potentials of the methyl and ethyl radicals. In that investigation,

---

* This work was supported by the U. S. Navy Bureau of Ordnance. A report on this work was presented at the Washington meeting (May, 1952) of the American Physical Society.

[1] A. G. Gaydon, *Spectroscopy and Combustion Theory* (Chapman and Hall, Ltd., London, 1948).

[2] G. C. Eltenton, J. Chem. Phys. **15**, 455 (1947).

[3] R. G. T. Fraser and T. N. Jewitt, Proc. Roy. Soc. (London), **A160**, 563 (1937).

however, lower source pressures were involved and detection of radicals was made with an ionization gauge.

The presence of atoms and free radicals in the molecular beam can be determined by appearance potential measurements[4,5] since their ionization potentials will be lower than the corresponding appearance potentials of electron dissociation products. If $A(X)$ is the appearance potential of the ion X^+ formed by dissociative ionization of the molecule XY by the electron impact process,

$$XY+e\rightarrow X^{+}+Y+2e, \qquad (1)$$

then

$$A(X)=D(XY)+I(X)+E, \qquad (2)$$

where $D(XY)$ is the dissociation energy of XY, $I(X)$ is the ionization potential of the radical X, and E is the sum of the kinetic and electronic excitation energies of X^+ and Y. Since dissociation energies are of the order of a few electron volts, it is possible, in principle at least, to detect radicals by employing electron energies slightly below the value required for the dissociative ionization process. In practice the thermal spread in energy of the bombarding electrons causes all observed ionization curves to vanish exponentially as the voltage is decreased. To resolve radicals from dissociative ionization products requires then that the electron voltage be chosen so that contributions from the tail of the dissociative ionization curve can be neglected. A consequence of operating at low electron energies is that the effective sensitivity of the mass spectrometer for radical detection may be reduced by perhaps a hundredfold from the sensitivity that is obtained if one operates at the maxima of the ionization efficiency curves, a situation which is approximated at conventional ionizing voltages (50 to 75 volts).

Another possible means of detecting free radicals, which avoids the difficulties due to dissociation effects at high electron energies, is to form negative ions by electron attachment. This method is not favored in the mass spectrometer because collisional stabilization of the excited negative ions is ruled out as a possible mechanism at the prevailing pressures in the ion source, and radiative capture of an electron is an inefficient process, the probability of capture in the case of atoms being about 10^{-7} per collision.[6] In the experiments to be described, no effort was made to detect radicals by the electron capture mechanism.

III. EXPERIMENTAL ARRANGEMENT

Figure 2 shows the actual physical arrangement of the gas inlet system employed in the flame studies. The burner section and the disk mounting the sampling orifice are clamped to the mass spectrometer with teflon gaskets employed for vacuum seals. To reduce scattering of the molecular beam in the first region, the second orifice (diameter 0.0286 in.) is drilled in a hollow conical brass piece which is threaded for movement in an axial direction. A magnetically driven beam chopper mounted ahead of the second orifice serves an important role in a scheme for discriminating against background signals. The second region is a noncritical transition section between the moderately high pressure (5×10^{-3} mm) in the first region and the high vacuum ($\sim10^{-6}$ mm) in the ion source. The third slit is a rectangular channel, with entrance dimensions 0.052 in. $\times$0.099 in., which diverges to prevent specular reflection of beam molecules into the ion source.

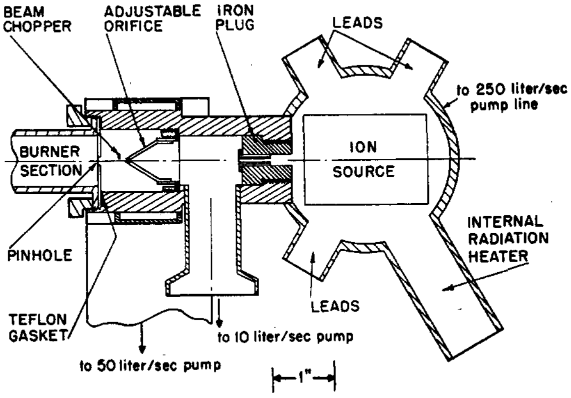

FIG. 2. Cross section of mass spectrometer gas inlet system.

A circular sampling aperture rather than a conventional narrow rectangular slit having the same gas capacity was adopted in these experiments to minimize reactions on the slit surfaces. It is likely that gas sampling systems designed in the future will utilize the recently described technique of producing a high intensity molecular beam[7,8] by placing the first slit in the supersonic stream of a miniature nozzle. The observed beam intensity, in our present design, is also considerably larger than expected for a conventional molecular beam design in which the slit width is limited to one mean free path.[9] The beam definition required in our case is much less than in most molecular beams so that cloud formation, which adversely affects the intensity of highly collimated beams, is not a serious factor. The simple sampling design employed here to study chemical reactions causes the reaction to be quenched very rapidly ($\sim10^{-6}$ sec) as the gas expands so that very active intermediates should survive extraction from the reaction zone.

The burner assembly is shown in Fig. 3. The reactants may be premixed or, as is indicated in the figure, sent in separately. The central burner tube is insulated from the rest of the assembly by a Teflon sleeve and can be moved by a micrometer drive mechanism. The

---

[4] J. A. Hipple and D. P. Stevenson, Phys. Rev. **63**, 121 (1943).

[5] D. P. Stevenson, Disc. Faraday Soc. No. 10, 35 (1951).

[6] H. S. W. Massey, *Negative Ions* (Cambridge University Press, Cambridge, 1950).

[7] A. Kantrowitz and J. Grey, Rev. Sci. Instr. **22**, 328 (1951).

[8] G. B. Kistiakowsky and W. P. Slichter, Rev. Sci. Instr. **22**, 333 (1951).

[9] R. G. J. Fraser, *Molecular Rays* (Cambridge University Press, Cambridge, 1931).

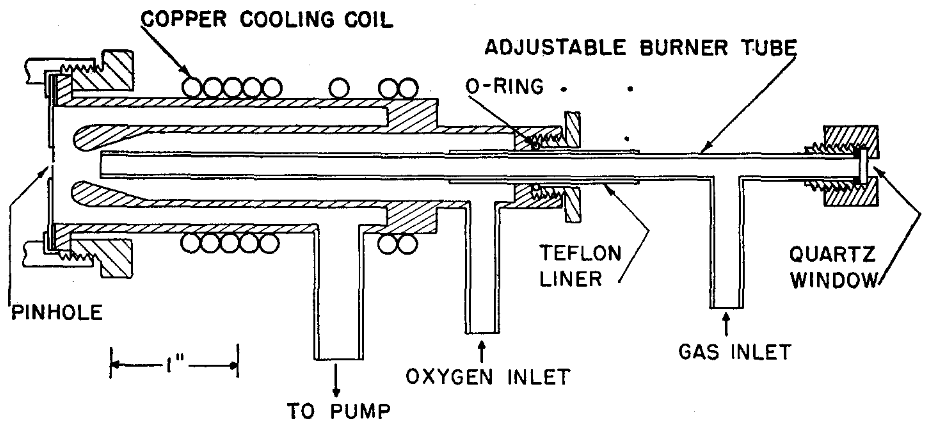

FIG. 3. Burner assembly.

flame is ignited by an electrical discharge between the center tube and the metal burner housing. A quartz window is used to observe the flame and to monitor the temperature of the diaphragm to prevent melting. The construction of the sampling orifice is shown in detail in Fig. 4. The diaphragm was usually a disk of gold foil 0.001 in. thick spotwelded, sandwich style, between the nickel welding ring and the monel plate. Approximately 50 spotwelds around the nickel ring were used to make a strong vacuum-tight joint. The entrance orifice was punched with a tungsten needle after the welding operation. Depending on the range of burner pressures to be explored the orifice diameter varied from 0.001 in. to 0.0045 in. The variation of ion beam intensity with pressure in the burner section is illustrated in Fig. 5 for oxygen entering through the 0.0045-in. pinhole. Since the scattering pressure in the first section is proportional to the burner pressure, and the unscattered molecular beam intensity is likewise proportional to the burner pressure, the ion intensity might be expected to follow the simple relationship $I\alpha pe^{-p/c}$, where I is the ion intensity, p is the burner pressure, and c is a constant. The theoretical curve shown was computed for $c=3.3$ cm Hg pressure. The maximum molecular beam intensity is normally obtained when the mean free path in the scattering region is just equal to the distance between the slits. Scattering of the beam near the entrance orifice will reduce the mean free path below the value computed from kinetic theory. In our case the distance between slits is 0.454 cm and the maximum intensity occurs at a chamber pressure of 4 microns. The mean free path for oxygen molecules from kinetic theory is 1.3 cm at 4 microns pressure, so that scattering in the beam and near the entrance slit has cut the effective mean free path by a factor of 3. It should be noted that the maximum beam intensity is obtained when the ratio of orifice diameter to mean free path in the burner, D/λ, is 70 rather than unity, which is the optimum value for conventional molecular beams.

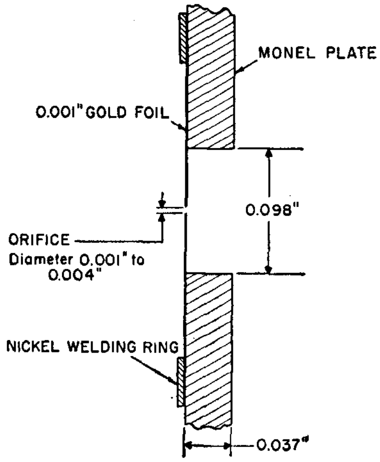

FIG. 4. Sampling orifice construction.

The operation of the mass spectrometer in obtaining data will be explained by referring to the block diagram of the instrument shown in Fig. 6. For exploratory work the beam chopper is not used, the ion accelerating energy is automatically swept with a sawtooth waveform, and the ion spectrum is displayed on an oscilloscope screen. A magnetically operated gate permits the selection of either a conventional electrometer amplifier (VX-41) detector, with a feedback circuit to reduce the input circuit time constant, or an electron multiplier detector. The electron multiplier detector with 13 stages of Be-Cu electrodes was patterned after the design by Allen[10] and shortly after installation had an over-all multiplication of 10^7. A molybdenum helix heater and a radiation shield surrounded the multiplier to permit bakeout while on the system. Comparison of the ion spectra obtained with the two detectors serves to determine (1) the relative sensitivity of the electron multiplier for different ions and (2) the current gain of the multiplier, a parameter which slowly decreased with time. Weak ion intensities are recorded by a conventional scaler circuit connected to the electron multiplier. The presence of background ion signals which arise from the diffusion pump oil, pyrolysis products generated by the filament, and diffusely scattered or reacted beam molecules seriously limit the useful sensitivity

---

[10] J. S. Allen, Rev. Sci. Instr. 18, 739 (1947).

of the detecting system thus far described. Dissociation products generated at the hot filament, even when an oxide cathode is used, are particularly annoying in experiments on atom and radical detection. By incorporating a molecular beam chopper between the first and second slits and employing phase detection of the ion current signal, the background problem is virtually eliminated. The beam chopper is a vibrating reed magnetically driven at a frequency of about 200 cps with amplitude stabilization derived from a capacity pickup in the feedback loop of the driver oscillator. A sylphon bellows allows some lateral displacement of the chopper to obtain a symmetrical wave form of the ion signal. The time constant of the phase detector recording circuit is 8 seconds. With the high pulsing rate of the molecular beam used here, the background pressure in the ion source, and consequently the background ion intensity, does not change materially between bursts. A moderately high chopping frequency is necessary to assure adequate discrimination against pyrolysis products of the molecular beam constituents. If the molecular beam is harmonically modulated at an angular frequency ω, the volume of the ion source housing and pumping line is V liters, and the speed of the diffusion pump is S liters/sec and if $\omega V \gg S$, one finds that the ion source pressure is fractionally modulated by $S/\omega V$ and the phase angle Φ is given by $\tan\Phi = \omega V/S$. The in-phase component of the pressure variation which is observed by the phase detector is thus S^2/ω^2V^2. In our case $\omega \sim 1200$/sec, $V \sim 5$ liters, and $S \sim 100$ liters/sec so that $\omega V \sim 60S$ and the in-phase component of the background pressure variation is about 3×10^{-4}. The effect of pressure modulation can be further reduced, if required, by slightly adjusting the phasing of the detector. Statistical fluctuation in the background signal level is generally a more important factor, particularly for small ion intensities.

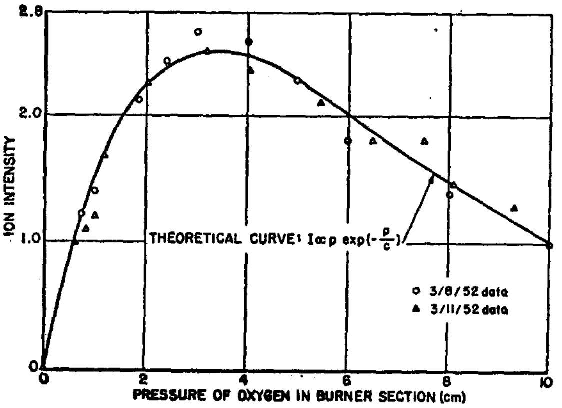

FIG. 5. Beam intensity as a function of pressure in the burner section.

In an experiment to determine the background discrimination which is actually realized by the beam modulation technique, an argon beam from the burner section which gave a detector signal of 3 millivolts, corresponding to about 400 ions/sec, was observed while a background pressure of argon was developed in the ion source by sending argon directly into the ion source through a needle valve. The modulated beam could be measured in the presence of a 40-volt dc background signal so that a discrimination factor of 10^4 was obtained. In the important practical case where the background arises from scattered beam molecules, including decomposition products formed on the filament, the collimation of the molecular beam introduces an additional discrimination factor of 10 because the molecular density in the beam is about 10 times the scattered molecular density in this apparatus. The signal-to-noise voltage ratio S/N for a system using a modulated beam when the noise results from statistical fluctuations in the background intensity is given approximately by

$$S/N = n(T)^{\frac{1}{2}}/(n_s)^{\frac{1}{2}}, \tag{3}$$

where n = the number of ions/sec from modulated beam, n_s = the number of disturbing ions/sec from the background, and T = observation time in seconds. If the background noise is developed primarily by scattering and reaction of certain beam constituents whose density in the primary beam is R times the density of the desired component and if each reaction generates α disturbing atoms or radicals, then

$$S/N \geq (nTc/\alpha R)^{\frac{1}{2}}, \tag{4}$$

where c is the beam collimation factor, with the equality sign representing complete conversion of the primary beam constituents. Experiments were performed with gases, such as hydrogen and oxygen which are known to react on the filament to produce hydrogen atoms and carbon monoxide, respectively, to see if the pyrolysis products would be observed with the chopped

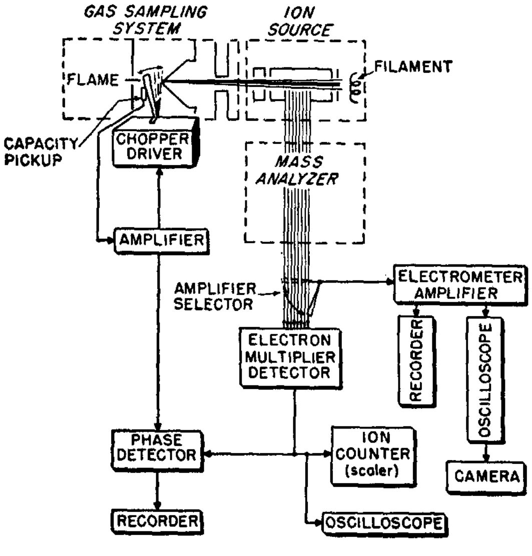

FIG. 6. Block diagram of the mass spectrometer.

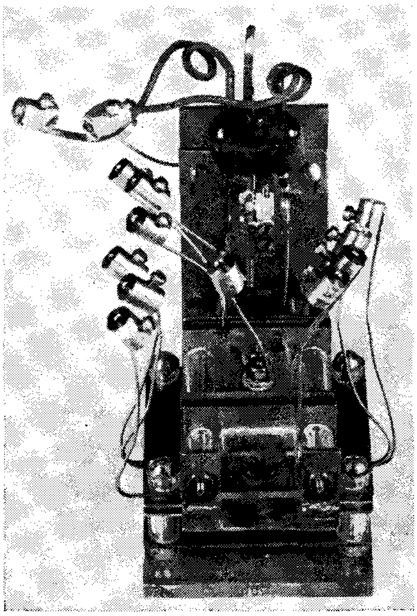

FIG. 7. Photograph of the ion source assembly showing the aperture through which the molecular beam enters.

beam method. No indications of decomposition products were observed.

The electron gun assembly with a view of the entrance hole in the last plate for the molecular beam is shown in Fig. 7. Because the electron and molecular beams are coaxial in the present design, the electron collector box was fabricated of mu-metal to cause the magnetic lineup field to vanish inside the collector box. The electrons are constrained to follow the magnetic field lines and run into the walls of the collector.

Mass analysis was performed in a 90° sectored magnetic field, using a 5-inch radius of curvature, and employing slits which gave a resolution of about 1 part in 130.

IV. EXAMPLES OF ATOM AND RADICAL DETECTION: H, OH

The appearance potential method for detecting atoms and radicals is illustrated in Figs. 8 and 9 for the cases of the hydrogen atom and the OH radical which were observed in the hydrogen-oxygen flame. An oxide-coated cathode was used as an electron source. The logarithmic plot of ion intensity in Fig. 8 indicates that H^+ ions come from two processes: (1) $H+e\rightarrow H^+ + 2e$, and (2) $H_2O+e\rightarrow H^+ + OH + 2e$ or $H_2+e\rightarrow H^+ + H + 2e$, with the onset energies separated by about 5 volts.† In Fig. 9 the OH^+ ions are formed by (1) $OH+e\rightarrow OH^+ + 2e$ and (2) $H_2O+e\rightarrow OH^+ + H + 2e$. The rough separation in onset energies is 5 volts in agreement with the theoretical lower limit, 5.17 volts, corresponding to the dissociation energy of the H_2O molecule. The appearance potential data taken with unstabilized flames as radical sources are not good enough for exact energy determinations. The same technique applied to atoms and radicals generated in high concentrations by a discharge tube source or by pyrolysis of compounds such as $Pb(CH_3)_4$ should yield results comparable to those normally obtained with stable molecules. It was not felt, however, that such measurements were required for the present investigation. It is evident that for electron energies at or below 18 volts the contributions from dissociation processes are negligible for both OH and H.

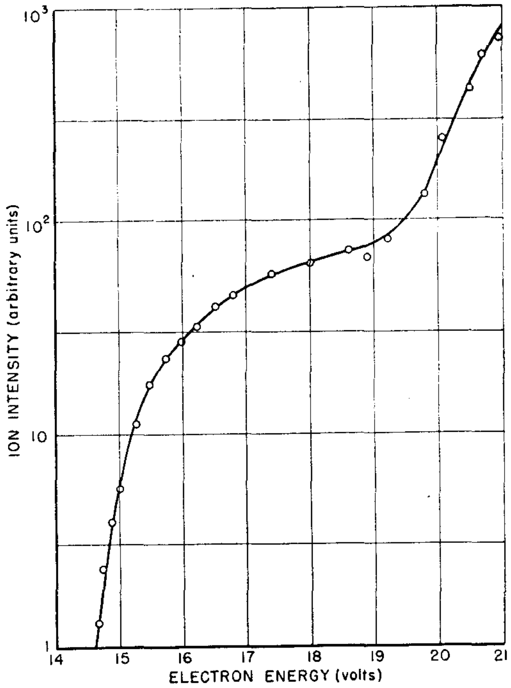

FIG. 8. Appearance potential curve for hydrogen atoms in the hydrogen-oxygen flame. Voltages are uncorrected for contact potentials, space charge, etc.

V. ANALYSIS OF FLAMES

Hydrogen-Oxygen Flame

The reaction of hydrogen and oxygen has been studied extensively[11,12] both experimentally and theoretically. Since a relatively small number of chemical entities can be present in the hydrogen-oxygen reaction, positive identification of the constituents can be obtained by mass analysis and appearance potential studies.

Low-pressure hydrogen-oxygen flames have been explored with the burner assembly previously described

---

† The experimental onset energy separation agrees somewhat better with the value for H_2 ionization [H. D. Smyth, Revs. Modern Phys. **3**, 347 (1931)], $18.6-13.53=5.1$ volts, than with the value for H_2O ionization, 6.0 volts.

[11] C. N. Hinshelwood and A. T. Williamson, *The Reaction between Hydrogen and Oxygen* (Oxford University Press, New York, 1934).

[12] B. Lewis and G. von Elbe, *Combustion, Flames and Explosions of Gases* (Cambridge University Press, New York, 1938).

(Fig. 3) in an effort to identify the reaction intermediates. The gases were admitted separately, hydrogen entering through the central burner tube and oxygen flowing in the surrounding annular space. Analyses of the mass spectra obtained with the modulated beam method clearly indicated the presence of H, O, and OH as intermediates. The intensities of these intermediates were in fact adequate to permit profile mapping of the flame as the central burner tube was moved away from the pinhole.

The observed ion intensities for a hydrogen-oxygen flame at 6 cm pressure with flow rates at NTP of 300 cc/min H_2 and 860 cc/min O_2 are given in Fig. 10. The stable components H_2, O_2, and H_2O are treated in the upper graph, while the intermediates are shown in the lower graph. The electron accelerating voltages were 48 volts for the stable components and 18 volts for the intermediates. The abscissa is the relative displacement of the burner tube from the pinhole with the origin corresponding to a minimum spacing of about 0.050 in. enforced by a mechanical stop to prevent the burner tube from being driven accidentally into the gold diaphragm.

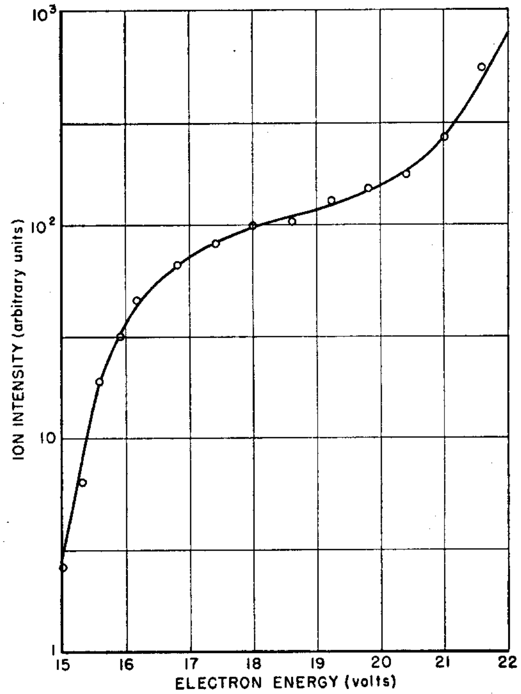

FIG. 9. Appearance potential curve for the OH radical in the hydrogen-oxygen flame. Voltages are uncorrected for contact potentials, space charge, etc.

The interpretation of the data is complicated by diffusion effects, turbulent mixing, and changes in the flame front configuration as the central tube is displaced. These curves are not, therefore, to be confused with the concentration profiles in a flame with premixed gases. Moreover, the diaphragm affects the hydrodynamic flow of the gases, a circumstance which is difficult to avoid and is probably the most serious deficiency of the gas sampling system design.

The discontinuities in the H_2 and H_2O curves at 0.025 in. were quite reproducible and accompanied by a change in the appearance of the flame. This probably means that the flame front has two stable positions and flips from one to the other at the discontinuity. The region 0.025 in. to 0.075 in. shows the classical behavior: H_2 and O_2 being consumed, H_2O being produced, and H, O, and OH going through maxima. The behavior of the various concentrations in region 0.075 to 0.250 in. may be interpreted as the result of continuous variation in the shape of the flame front as the burner tube is retracted. The O_2 and H_2O concentrations are almost mirror images, an increase in one accompanied by a decrease in the other. Since the atom and radical concentrations do not follow the concentration changes of the stable components, we conclude that they are produced primarily by chemical kinetic mechanisms rather than by dissociation of the stable components at the flame temperature.

The determination of absolute concentrations of H, O, and OH would require that the mass spectrometer be calibrated with sources of these intermediates in which the concentrations could be computed from thermodynamic data (for example, thermal dissociation of H_2O at high temperatures) or measured by inde-

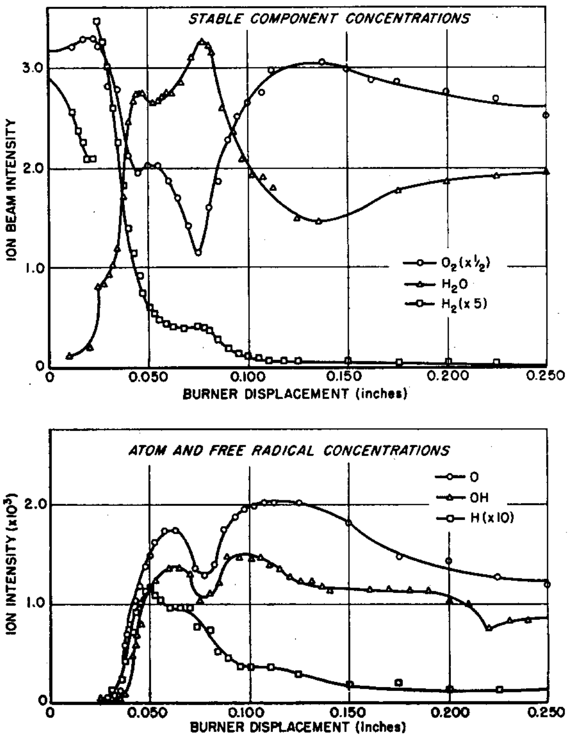

FIG. 10. Ion intensity measurements of stable components and intermediates in the low pressure hydrogen-oxygen flame. The abscissa is the relative displacement of the central burner tube from the pinhole.

pendent means (for example, absorption spectroscopy for OH). In the absence of such a calibration in our work to date, an order of magnitude estimate of the radical concentrations may be made by assuming that their ionization cross-section curves are similar to those of their associated stable molecules. On this basis the intensities of the curves in the lower graph of Fig. 10 should be multiplied by about a factor of 10 when compared with the upper graph to compensate for the decreased sensitivity at the lower electron energy. The maximum atom and radical concentrations are thus estimated to be of the order of 1 percent.

One of the principal reasons for studying the H_2-O_2 flame was the possibility of obtaining direct experimental evidence of the existence of the HO_2 radical[13,14] which has been postulated as a reaction intermediate to explain the second and third explosion limits. In principle, the experimental conditions for HO_2 detection are much better than for the detection of the other intermediates, since the only interfering peaks at mass 33 are $O^{16}O^{17}$ present as 0.078 percent of the O_2 concentration and possibly HO_2^+ from dissociative ionization of H_2O_2. Under experimental conditions in low pressure flames which afforded a generous yield of H, O, and OH a search was made for HO_2 at mass 33 and H_2O_2 at mass 34. In these experiments no excess in the 34 peak above the expected $O^{16}O^{18}$ intensity was observed so that H_2O_2 dissociation did not contribute to the 33 peak. Under these conditions observations can be made both at high electron energies to see if there is an excess of mass 33 above the $O^{16}O^{17}$ value and at low electron energies to see if an ion current is obtained below the appearance potential of the molecular oxygen ion on the assumption that $I(HO_2)<I(O_2)$. The results of the low electron energy experiments were negative. At high electron energies there was a small increase in the 33 peak intensity, although the change was not outside the limits of error in our measurement of the 33/32 ratio. Attempts to adjust flame parameters such as burner position, burner pressure, and hydrogen-oxygen ratio to increase the 33 peak were uniformly unsuccessful. For some unknown reason the reproducibility of the measurements of the $O^{16}O^{17}/O_2^{32}$ ratio made at different times was not so good as for other isotopic ratios. The excess in mass 33 was definitely less than 0.01 percent of the O_2^{32} intensity and was therefore at least a hundredfold smaller than the observed OH intensity.

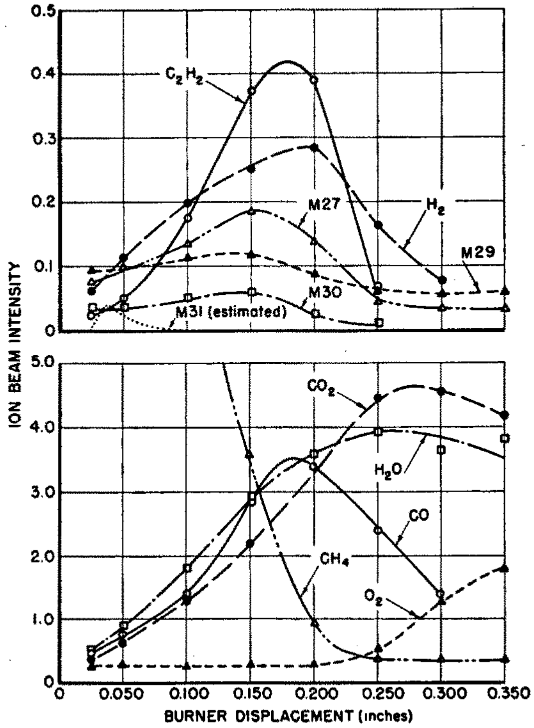

FIG. 11. Ion intensity measurements of the major components in a low pressure methane-oxygen flame. The data were obtained by photographing oscilloscope presentations of the mass spectra and are uncorrected for background. The abscissa is the relative displacement of the burner tube from the pinhole.

It was felt that our failure to observe HO_2 in low pressure flames could be explained by the requirement of triple collisions for HO_2 formation which would be favored by higher pressures. Consequently a few experiments were made with a smaller sampling pinhole (0.001-inch diameter) which permitted higher burning pressures. Burning at pressures up to 0.5 atmosphere did not give positive indications for the HO_2 radical. In order to clarify the situation of the HO_2 radical a series of experiments are being planned in which hydrogen atoms from a Wood's discharge tube are allowed to react with oxygen molecules.‡

Methane-Oxygen Flame

The primary purpose in presenting the data for the methane-oxygen flame is to indicate the complexity of the reaction system which obtains in a hydrocarbon flame and to point out some of the analytical difficulties which result from this situation. In studying the methane-oxygen flame, one essentially investigates the general problem of hydrocarbon combustion because a number of the intermediates found are higher mass hydrocarbons, alcohols, etc. Whereas the identification of a component by mass number is quite adequate in simple reactions, such a procedure is insufficient and can easily lead to incorrect results in hydrocarbon flames. The detection of radicals is also made difficult because a large number of molecules are potential sources of the radical ion in dissociative ionization processes.

The combustion of methane, the simplest hydrocarbon, was used in our early experiments to check out

---

[13] C. N. Hinshelwood, Proc. Roy. Soc. (London) A188, 1 (1946).

[14] G. J. Minkoff, Disc. Faraday Soc. 2, 151 (1947).

‡ *Note added in proof.*—These experiments are reported in a letter to be published in this journal entitled "The Detection of the HO_2 Radical by Mass Spectrometry."

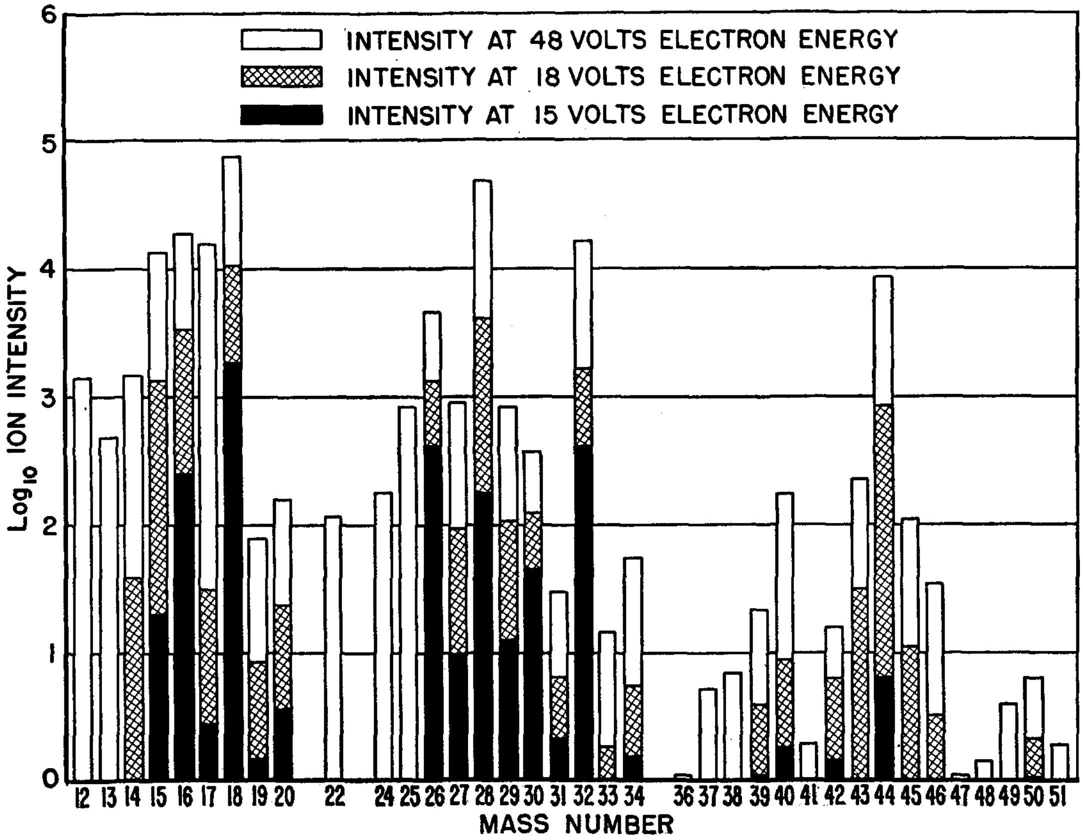

FIG. 12. Mass spectra of the methane-oxygen flame obtained at different values of electron energy. A range of 10^6 in intensities is covered by the logarithmic scale. The actual electron energies are lower than the indicated voltages by about 1.5 volts because of contact potentials, space charge, etc.

the molecular beam sampling techniques. Figure 11 shows the composition profiles for the major peaks in the CH_4-O_2 flame at 12 cm pressure when methane was admitted in the center tube and oxygen flowed in the surrounding annulus. In this particular experiment, which was made prior to the installation of the beam chopper, the sampling orifice was a 0.002-in. hole in an 0.002-in. platinum diaphragm, and the ion spectra were displayed on an oscilloscope screen and photographed. As the burner tube is displaced from the pinhole the decrease in CH_4 is accompanied, as expected, by increases in CO_2, H_2O, and O_2. The curves for CO, C_2H_2, H_2, and components having masses 27, 29, 30, and 31 go through distinct maxima showing that they are formed in the early stages of the reaction and are consumed as the reaction goes to completion. The large amount of acetylene produced in the reaction shows that the combustion reaction is by no means simple. The ion intensities at the numbered masses have been corrected for contributions from the other components and have been tentatively identified as follows: mass 27, $C_2H_3^+$ from C_2H_4; mass 29, CHO^+ from HCHO or $C_2H_5^+$ from C_2H_6; mass 30, $C_2H_6^+$ or $HCHO^+$; mass 31, CH_3O^+ from CH_3OH.

The complexity of the methane-oxygen combustion spectrum poses some formidable analytical problems. This situation is illustrated in Fig. 12 which gives recent data for combustion at 0.1 atmosphere obtained at a single burner position with the modulated beam technique. The gas sampling orifice in this case was a 0.004-in. hole in the usual 0.001-in. thick gold diaphragm. Ion spectra were measured at different electron bombarding energies not only to furnish evidence for radicals in the flame but to provide some analytical assistance in interpreting the spectrum. Despite the assistance rendered by variations in pattern with electron energy, it has not been possible to identify the sources of all the ion peaks shown. The difficulty in making identifications stems from the following sources: (1) there are a large number of chemical compounds which could conceivably be manufactured from the reactants and give peaks at the observed mass numbers; (2) some of the molecules extracted from the flame are in excited states and therefore will have dissociative ionization spectra which are different from standardizing spectra obtained at normal temperatures; (3) unstable components whose ion spectra can only be guessed are also present.

The intensity measurements at the lowest energy (15 volts) are of particular importance because most of the peaks correspond to parent ions, thus simplifying the picture considerably. In the low energy mass spectrum of Fig. 12 the following stable components can be readily identified: CH_4, H_2O, C_2H_2, CO_2, O_2, CO_2, C_4H_2. Certain other stable compounds are certainly present although there is some ambiguity in the assignments. For example, the mass 30 peak is contributed by formaldehyde or ethane or a mixture of both. Resolution of the formaldehyde-ethane question by examination of the 27 peak which is characteristic of ethane is not possible because other hydrocarbons in the spectrum have mass 27 dissociation products. The situation in the upper portion of the mass range shown in Fig. 12 is not too clear, although the data suggest that C_3H_4, C_3H_6 and C_3H_8 are present.

In examining the spectrum for evidence of free radicals one initially assumes that all observed peaks arise from stable compounds. There must be convincing evidence that a peak could not be generated by ionization or dissociation of stable molecules before it is attributed to a radical. The only radical in the methane-oxygen flame for which we have positive proof at this time is the CH_3 radical. In addition to observing a large intensity at mass 15 (see Fig. 12) which could not be due to anything other than the CH_3 radical, we have appearance potential data which substantiates this identification. Appearance potential curves have not been obtained for the components at masses 29, 31, and 39 which might be expected to disclose the presence of the radicals HCO or C_2H_5, CH_3O, and C_3H_3, respectively. The CH_3O^+ intensity at mass 31 ostensibly comes from methyl alcohol ionization. Although the intensity of C_3H_3 cannot come from propane[15] [$A(C_3H_3^+)=15.7\pm0.5$ volts] or propylene[15] [$A(C_3H_3^+)=14.1\pm0.2$ volts], and is too high to be expected from C_3H_4 ionization, we do not have definite proof for the presence of the C_3H_3 radical since an appearance potential curve for the ion was not obtained. A similar situation exists in the case of the mass 29 peak.

The intensity of mass 33 at 15 volts (too small to appear on the graph, Fig. 12) was higher than the $O^{16}O^{17}$ contribution from oxygen, while the mass 34 peak checked the expected $O^{16}O^{18}$ intensity. The isotopic contribution from methyl alcohol is probably not sufficient to account for the discrepancy. We are reluctant to ascribe the small intensity difference to the HO_2 radical, particularly in view of our essentially negative results for this radical in the hydrogen-oxygen flame. In the complicated methane-oxygen flame it is possible that the small excess in the ion peak at mass 33 could even be CH_5O^+ which occurs as a large peak in the spectrum of isobutyl alcohol.[16]

VI. DISCUSSION

The negative result for the HO_2 radical in the hydrogen-oxygen flame is not due to an instability of the HO_2^+ ion since this ion occurs in the mass spectrum of hydrogen peroxide. The interpretation of Eltenton's[17] observed intensities at mass 33 in the methane-oxygen and propane-oxygen flames is not clear. Identification of his mass 33 peak as HO_2 must be treated with reservations in view of some alternative explanations for intensity at this mass number, particularly since his system was unable to detect the OH radical in flames. The experiments reported here do not, however, rule out the occurrence of the HO_2 radical in the hydrogen-oxygen flame in considerably smaller concentration than the other intermediates.

The difficulty in identifying the intermediates in hydrocarbon flames, illustrated in the case of the methane-oxygen flame, arises from the complexity of the spectrum due to the large number of compounds present in the flame, rather than from an intrinsic inability to distinguish the radicals from the stable components. In most cases where the ion intensities are high enough to permit good determinations of appearance potentials, the ambiguity between radicals could be resolved. The appearance potentials of the free radicals would, of course, have to be determined by other experiments, such as electron impact studies of stable molecules. It should be noted that the appearance potential method for detection can not be applied if the ionization potential of the atom or radical is greater than that of a stable constituent of the system which is present in high concentration. For example, oxygen atoms ($I.P.=13.63$ volts) would not be detected in the presence of methane ($I.P.=13.1$ volts). A practical solution to this problem lies in utilization of mass spectrometers with higher mass resolution. The use of an instrument with higher resolving power would also solve some of the analytical problems in identifying the stable components in complex reactions.

At the present time it appears that the most profitable applications of the mass spectrometric techniques for detecting atoms and free radicals will be in elucidating the mechanisms of simple gas phase reactions. There are a number of interesting reactions between atoms and molecules which have been studied with less definitive analytical methods.[18] Among the elementary reactions which we propose to investigate in detail is the reaction of hydrogen atoms with oxygen molecules.

The authors are indebted to Dr. F. T. McClure, Dr. W. H. Avery, and Dr. A. Kossiakoff for advice and encouragement during the course of the investigation and to Mr. B. H. Nall for building the electron multiplier detector.

---

[15] J. Delfosse and W. Bleakney, Phys. Rev. **56**, 256 (1939).

[16] Mass Spectral Data, API Research Project 44, National Bureau of Standards Serial No. 369.

[17] Reference 2, page 478.

[18] E. W. R. Steacie, *Atom and Free Radical Reactions* (Reinhold Publishing Corporation, New York, 1946).